Original Research Article

Development of Curcumin loaded Nanostructured Lipid Carriers: Preparation, Characterization and *In-vitro* evaluation of Anti-cancer activity against A-549 Human lung cancer cell line

.

ABSTRACT

Aims: The present study was aimed at preparing stable lyophilized curcumin loaded nanostructured lipid carriers (NLCs). The optimized lyophilized curcumin loaded NLCs were characterized and evaluated for various quality control parameters.

Methodology: The optimized curcumin loaded NLCs were prepared by modified hot emulsification using compritol 888 ATO (CMPR), capmul MCM C8 EP (CAP) as solid and liquid lipids respectively. The combination of tween 80 (T80) and solutol HS 15 (SHS) were used as an emulsifier. The NLCs dispersion was lyophilized into powder form to improve the thermodynamic stability of the formulation. The lyophilized curcumin loaded NLCs were evaluated for particle size, size distribution, zeta potential, entrapment efficiency (EE), drug loading, assay, *in-vitro* drug release, crystallinity, thermal behavior and surface morphology studies.

Results: The optimized lyophilized curcumin loaded NLCs have a mean particle size of 332.88 ± 5.9 nm with a size distribution of 0.350 ± 0.007, a zeta potential of 0.098 ± 0.019 mV with high entrapment of 97.64 ± 1.59 % and drug loading of 2.50 ± 0.16 %. The X-ray diffraction and endothermic peaks confirmed the maximum encapsulation of curcumin in lipid matrices. The particles were spherical with smooth surface morphology. *In-vitro* release studies showed sustained release for up to 24 h. The cytotoxicity against human lung cancer line A-549 for curcumin loaded NLCs was confirmed with positive control adriamycin (ADR).

Conclusion: Curcumin loaded NLCs prepared had a nanosize particle distribution with maximum entrapment efficiency. Dispersion stability was increased by the lyophilization process. The solid lyophilized powder is reconstituted for oral delivery.

Keywords: Curcumin, Nanostructured lipid carrier, Lyophilization, Anti-cancer activity.

1. INTRODUCTION

Curcumin, a polyphenolic molecule, targets many signaling components at the cellular level [1]. Curcumin is a natural product that has a lot of potential for cancer treatment because it is safe, cheap, and easy to available. Curcumin has a strong intracellular effect, affecting processes such as genome modification, cell invasion, and cell death. As a result, curcumin appears to be a viable cytostatic and cytotoxic agent. Curcumin inhibits transcription factors and downstream gene products, has antiproliferative effects, affects growth factor receptors, changes cell adhesion molecules in angiogenesis, inhibits inflammatory cytokines, and inhibits protein kinases, all of which affect tumor growth and metastasis. Recent literature

has reported cytotoxic activity potentially due to telomerase inhibition [2,3]. Curcumin uptake is higher in cancer cells than in normal cells due to reduced glutathione levels in cancer cells, which increases their sensitivity to curcumin [4]. Curcumin did not affect normal rat hepatocytes in terms of superoxide generation or cell death. Curcumin, as a result, has no cytotoxic effect on normal cells [5,6]. In healthy human volunteers, oral administration of 2 g of pure curcumin resulted in a plasma concentration of less than 10 ng/ml at 1 h post dose. The low plasma levels of curcumin are due to poor solubility and high first pass metabolism, as well as intestinal metabolism including glucuronidation and sulfation [7,8]. Curcumin's major degradation products are ferulic acid and vanillin, both of which have biological activity, including cytotoxicity [9]. Due to curcumin's poor aqueous solubility and bioavailability, the use of lipophilic substances in lipid-based nanosystems can improve solubility and bioavailability. Published literature showed the cytotoxic activity of curcumin loaded NLCs was evaluated against human HepG2 cells [10], U373MG astrocytoma–glioblastoma cell line [11], Caco-2 cells [12], brain cancer [13,14], HeLa cells [15], and A549 human lung adenocarcinoma cells [16]. In the present study, we evaluated *in-vitro* cytotoxic activity against cell lines of non-small cell lung cancer for an optimized curcumin-loaded NLC formulation.

2. MATERIAL AND METHODS

2.1 Materials

Curcumin of purity 99.50 % was obtained from VAV Life Science (Mumbai, India) as a gift sample. Compritol 888 ATO (CMPR), Geleole (GLE), Labrafac lipophile WL 1349 (LAF), Capryol PGMC (CPR) were gift samples obtained from Gattefosse, India. Dynasan 114 (D114), Dynasan 116 (D116), Dynasan 118 (D118), Miglyol 812 (MIG) were gift samples obtained from Cremer Oleo GmbH & Co. Germany. Capmul MCM C8 EP (CAP) was a gift sample obtained from Indchem International, India. Tween 80 (T80), Polaxomer 188 (P188), Solutol HS 15 (SHS), Kolliphore EL (KEL), Kolliphore RH 40 (KRH40) were gift samples obtained from BASF, India. Sesame oil, olive oil, rice bran oil, sunflower oil, cotton seed oil, coconut oil, mustard oil and wheat germ oil were purchased from Kamani oil Industries, India. Stearic acid, Palmitic acid and soyalecithin were purchased from Lobachemie, India. Mannitol (Pearlitol 200SD) and Dextrose (dextrose monohydrate GC) were obtained from Roquette, India. as a gift sample. Directly compressible sucrose (Compressuc PS) was obtained from Tereos, France as a gift sample. The methanol used was of high-performance liquid chromatography (HPLC) grade and obtained from LOBA-Chemie. Millipore (ultrapure) water was used for the preparation of all solutions.

2.2 Formulation development of lyophilized curcumin loaded NLCs

2.2.1 Screening of excipients

A semi-quantitative method was used to test the solubility of curcumin to screen for suitable formulation excipients. The solid lipids were melted at a temperature 5 °C above their melting point, and curcumin was added to the molten mass before being mixed in a vortex mixer (Remi CM 101 Plus; Remi Labs, India) to ensure uniform mixing and determine the maximum amount of curcumin that could be dissolved in each lipid. These solutions were visually checked for the presence or absence of curcumin, and the process was repeated until the lipid was saturated with curcumin. The lipid with the highest solubility for curcumin was chosen for further research [17]. Liquid lipid, emulsifier, and the ratio of solid lipid to liquid lipid were all screened using a similar approach (heating was applied for only solid components) [18].

2.2.2 Method of preparation

In modified hot melt emulsification, the curcumin was completely solubilized in the emulsifier. To this preconcentrate, liquid lipid and solid lipids were added to form a lipid phase. This preconcentrate is warmed to a temperature of 5 °C above the melting point of the solid lipid. On the other hand, purified water is placed on a preheated magnetic stirrer (Remi Ltd., India) at the same temperature. Then the preconcentrate is added to the purified water maintained at the same temperature under stirring. This mixture is kept on the magnetic stirrer (Remi Ltd., India) until a uniform emulsion is obtained (Fig. 1) [19]. Further particle size reduction was carried out using a probe sonicator (Oscar Ultrasonics Pvt. Ltd., India) with a 3 mm horn with a 30-40% variac and 90-watt power.

2.2.3 Formulation design for preliminary screening of formulation and process related parameters

Formulation parameters such as solid lipid and emulsifier concentration, as well as process parameters such as sonication time, were taken into account [18,20]. After each parameter screening, the best value of the parameter was finalized and kept as a constant for the next parameter screening (Table 1). All of the formulations had been prepared in triplicates.

Table 1. Preliminary screening parameters for curcumin loaded NLCs

Parameter	Preliminary screening	Variables
Curcumin	8 mg	
Solid lipid	1.2 % w/v	GMS, CMPR, D114, D116, D118
Liquid lipid	0.8 % w/v	CAP
Emulsifier	T80, SHS, T80+ SHS 15 (1:1)	
Emulsifier concentration (EC)	1.5 % w/v	1 %, 1.5 % , 2 % w/v
Purified water	10 ml	
Sonication time (ST)	10 min	5, 10, 15 min

2.2.4 Optimization - design of experiment

A 2-factor 2-level full factorial design was used for the optimization. The effect of formulation variables on the responses was statistically evaluated by applying one-way analysis of variance (ANOVA) using the software package Design Expert® version 9.0.3 (Stat-Ease Inc., Minneapolis, MN, USA). This helps to understand the combined effect of formulation and process related parameters. The influence of two independent variables, constituted of a formulation and a process-related parameter, emulsifier concentration (A: X1) and sonication time (B: X2) on the responses of particle size (Y1) and polydispersity index (PDI) (Y2) was studied. Each independent variable was varied at two levels: low (-1) and high (+1) (Table 2 and 3). Experimental trials were carried out in triplicates.

Table 2. Factorial design for optimization of curcumin loaded NLCs

Level	Factors A:X1 EC (mg)	 B:X2 ST (min)	Response Y1	 Y2
Low (-1)	130	7	Particle size	Polydispersity
High (+1)	180	12	(nm)	index (PDI)

Table 3. Factorial design layout for optimization of curcumin loaded NLCs

Runs	Batch code	A:X1, EC Level	Mg	B:X2, ST Level	min
1	F1	-1	130	-1	7
2	F2	-1	130	-1	7
3	F3	+1	180	-1	7
4	F4	+1	180	-1	7
5	F5	-1	130	+1	12
6	F6	-1	130	+1	12
7	F7	+1	180	+1	12
8	F8	+1	180	+1	12

Multiple regression analysis: The use of regression analysis in 2^2 factorial designs generates different polynomial equations for different models, with interacting terms and regression coefficients, useful in evaluating the responses. The software generates two models, a full model (non-significant terms included) and a reduced model (excluding non-significant terms). In the full model study, the responses were analyzed using the quadratic equation below:

$$Y = b_0 + b_1A + b_2B + b_{12}AB + b_{11}A^2 + b_{22}B^2$$

Y is the arithmetic mean response of eight runs; b_0 is the estimated coefficient of independent variables. The main effects (A and B) represent the average result of changing one factor at a time from its low to high value. The interaction term (AB) shows how the response changes when 2 factors are simultaneously changed. The polynomial terms (A^2 and B^2) were included to investigate nonlinearity.

Response surface methodology: It helps to quantify the relationship between one or more measured responses and the vital input factors. It helps in the determination of a desirable location in the design space. This space could be maximum, minimum or an area where the response is stable over a range of factors. A statistical relationship in the form of equations is obtained which shows the effect of varying A and B on the dependent variables, Y1 and Y2. In addition, contour and 3D surface plots were obtained by Design-Expert, to represent the effect of the independent variables graphically.

Identification of optimal batch: To determine the optimal batch, the fitted mathematical model was put in use. The two equations derived, i.e. for PDI (Y2) and particle size (Y1) in terms of X1 and X2, were sequentially employed. The formulation with the desirability value closer to unity is chosen as the optimized formulation. For the purposes of this study, the criteria for the optimum batch were chosen to be those with the smallest particle size and the lowest PDI.

2.2.5 Lyophilization

Solid dosage forms are more stable and preferred in nanoparticle formulations than liquids. Water must be removed from liquid systems to improve the physical and chemical stability of the nanoparticle system. In the present study, a few Cryoprotectants like dextrose, sucrose and mannitol were evaluated for lyophilization. These Cryoprotectants were screened at different concentrations (5,7 and 10%). The curcumin loaded NLC dispersions were frozen in aqueous cryoprotectant solution at-35 to-40 ℃ for about 24 h and then the samples were transferred to the lyophilizer (Biocryos, Korea) operated at-35 to-22 ℃ and a pressure of 200-500 millitorr for 24 h to obtain the finely dispersed NLC powders (Fig. 1). To assess the

redispersibility of lyophilized NLC, the grade system was used: Grade A: Quickly redispersible (15 sec, clear solution), Grade B: Moderately redispersible (> 15 sec, clear to translucent solution), Grade C: Poorly redispersible (does not redisperse, presence of large particles).

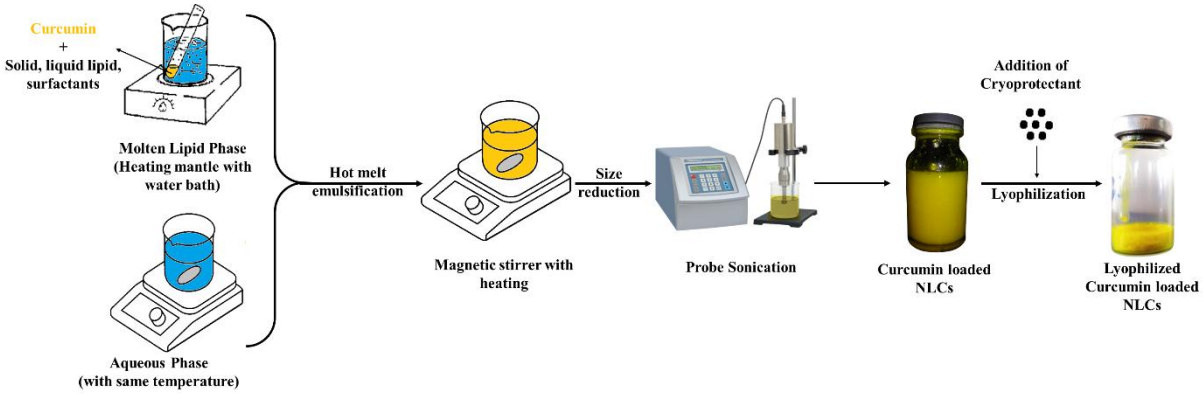

Fig. 1. Preparation of lyophilized curcumin loaded NLCs

2.3 Characterization and evaluation of lyophilized curcumin loaded NLCs

2.3.1 Redispersibility and drug content

An equivalent amount of water was added to the lyophilized product to maintain the concentration of the drug uniformly. The ability of the lyophilized powder to reconstitute into a uniform solution was observed. To extract the curcumin from the nanoparticles, 1 ml of curcumin loaded NLCs was diluted with methanol and sonicated for 60 min in a bath sonicator (Remi Ltd., India). The solution was filtered through a 0.45 µm nylon syringe filter, and the sample solution was diluted with the mobile phase to a final concentration of 10 µg/ml. This solution was then injected into the HPLC system, and the chromatogram was recorded as described in our previously published technique [21]. The following formula was used to compute the percentage assay or recovery of the sample solution:

$$\text{Recovery } (\%) = \frac{Amount\ of\ curcumin\ recovered}{Amount\ of\ curcumin\ added} \times 100$$

2.3.2 Particle size, size distribution and zeta potential

The Malvern Zetasizer ZS90 (Malvern Instruments, UK) was used to measure particle size and extent of size distribution (PDI) of curcumin NLCs at a 90° scattering angle using dynamic light scattering (laser beam of 633 nm). The samples were measured at a fixed angle of 90° at 25°C for light scattering measurements. By diluting the sample with double distilled water, the scattering intensity was varied between 100 and 500 kcps. Malvern Zetasizer ZS90 laser doppler micro-electrophoresis was used to determine the zeta potential (Malvern Instruments, UK). By inserting the samples in disposable zeta cell cuvettes and placing them in the sample chamber of the ZS 90, the zeta potential was determined.

2.3.3 Entrapment efficiency and drug loading

The EE of curcumin loaded NLCs was determined by an indirect method wherein the amount of unincorporated (unentrapped) curcumin in the aqueous phase of NLCs was determined. Curcumin NLCs and 0.9% sodium chloride solution at a ratio of 2:1 (v/v) was

subjected to centrifugation using a high speed centrifuge (Remi Ltd., India) at 14 000 rpm for 30 min to salt out the unincorporated curcumin. The upper portion of the sample was separated. 0.5ml of this solution was further diluted with methanol and the amount of the curcumin present was analyzed using an HPLC system [21].

$$\text{Entrapment efficiency (EE)}(\%) = \frac{Wt - Wa}{Wt} \times 100$$

$$\text{Drug loading}\ (\%) = \frac{Wt - Wa}{(Wt - Wa) + Wl} \times 100$$

Where, Wt stands for the total amount of curcumin added to the system, Wa stands for the amount of curcumin quantified by indirect method, WI stands for the amount of lipid.

2.3.4 Surface morphology

Scanning electron microscopy (SEM) (Philips XL30 FEG, Netherlands) was used to record the exterior surface morphology of curcumin-loaded NLCs at a voltage of 15 kV. The samples were double-sided adhesive taped on an aluminum stub. To make the sample conductive, a tiny layer of gold was sputter deposited on the stub containing the sample. After that, the material was examined at various magnification levels (8000x).

2.3.5 Crystallinity studies

The PAN analytical X'Pert PRO MPD (Multi-Purpose Diffractometer) System was used to measure the X-ray diffractogram (XRD) of lyophilized curcumin loaded NLCs. After loading the samples into an X-ray diffractometer, the spectrum range of 0-5000 intensity was detected at 2°. Pattern treatment, peak detection, and peak labelling were all done with PANalytical X'PertHigh Score software. Curcumin, solid lipid, and lyophilized curcumin loaded NLC formulations were all studied.

2.3.6 Thermal behavior

The Differential scanning calorimetric (DSC) analysis was performed using a DSC 7 Perkin Elmer differential calorimeter (PerkinElmer, Inc, USA). An accurately weighed amount of sample, i.e., curcumin, solid lipid, lyophilized curcumin loaded NLCs, was placed in 40 µl aluminum pans and analyzed. DSC scans were performed at a heating rate of 5 K/min from 30 °C to 250 °C and back to 25 °C, using an empty pan as a reference.

2.3.7 *In-vitro* drug release studies

The *in-vitro* drug release studies from redispersed curcumin lipoidal nanoparticles were performed using the dialysis bag (molecular cut-off of 12-14 kilo Dalton, Sigma-Aldrich Co., India) method [22]. The adequate volume of dissolution media, constituted of pH 6.8 phosphate buffer saline and ethanol in a ratio of 1:1, was maintained at 37℃ with agitation of 100 rpm. Aliquots volumes were withdrawn and replaced with fresh buffers at predetermined time intervals. Appropriate dilutions were made and the concentration of the curcumin was analyzed using the HPLC system [21].

To study the release kinetics, data obtained from *in-vitro* permeation studies was fitted in various kinetic models:

- The plot of cumulative percent of drug release versus time in zero order.
- The plot of the log of the cumulative percentage of drug released versus time is first order.

- Higuchi's model as the cumulative percent drug release versus square root of time.

The linearity of the plots or the R^2 values (coefficient of correlation) was calculated from the plots by regression analysis to determine the best fit model. To determine the mechanism of drug release, the data was fitted into the Korsmeyer Peppas model as the plot of log cumulative percentage of drug released versus log time, and the diffusion exponent n was calculated from the slope of the straight line. The diffusion exponent is 0.5, then the diffusion mechanism is fickian; if 0.5< n <1.0, the mechanism is non-fickian, n = 1 to case II (relaxational) transport, and n > 1 to super case II transport.

2.4 *In-vitro* cytotoxicity study for curcumin loaded NLCs

In-vitro cytotoxicity studies were carried out using the A-549 cell line, a representative cell line of non-small cell lung cancer, to evaluate the efficiency of curcumin against lung cancer. The studies were performed to check the effectiveness of nano formulated curcumin over standard curcumin in preventing cell growth. Analysis was carried out using three different samples. Curcumin loaded NLC formulation, curcumin dispersed in water, and curcumin in dimethyl sulfoxide (DMSO) were among the samples tested. A positive control ADR was also used to confirm that the cell line was itself significant for the studies. The samples were appropriately diluted to attain concentrations of 10, 20, 40 and 80 µg/ml. These solutions were incorporated into cultured cell lines and observed for anti-cancer activity.

2.5 Real-time stability studies

The optimized lyophilized curcumin loaded NLCs formulation was filled in aluminum polyvinyl chloride (Alu-PVC) sachets and subjected to different conditions (25 °C ± 2°C/60% ± 5% RH and 5 ± 3 °C) for stability studies over a three months according to international council for harmonization (ICH) guidelines. The formulations were evaluated for various quality control parameters.

3. RESULTS

3.1 Formulation development of lyophilized curcumin loaded NLCs

3.1.1 Screening of excipients

The solubility of curcumin in solid lipids is in the order of CMPR > D116 > GLE > D114 > D118. Palmitic and stearic acids were discontinued for further study due to their low solubility in curcumin. Curcumin solubility was higher in LAF>CPR>CAP>LBR>MIG than in other oil components. Further, it was observed that the maximum amount of curcumin was soluble in a blend of CMPR and CAP in a ratio of 60:40 when compared with various other solid lipid and liquid lipid combinations. Curcumin was degraded when added to emulsifiers KRH 40 and KEL. P188 had the least solubility (Fig. 2). Hence, T80 and SHS were taken for further studies.

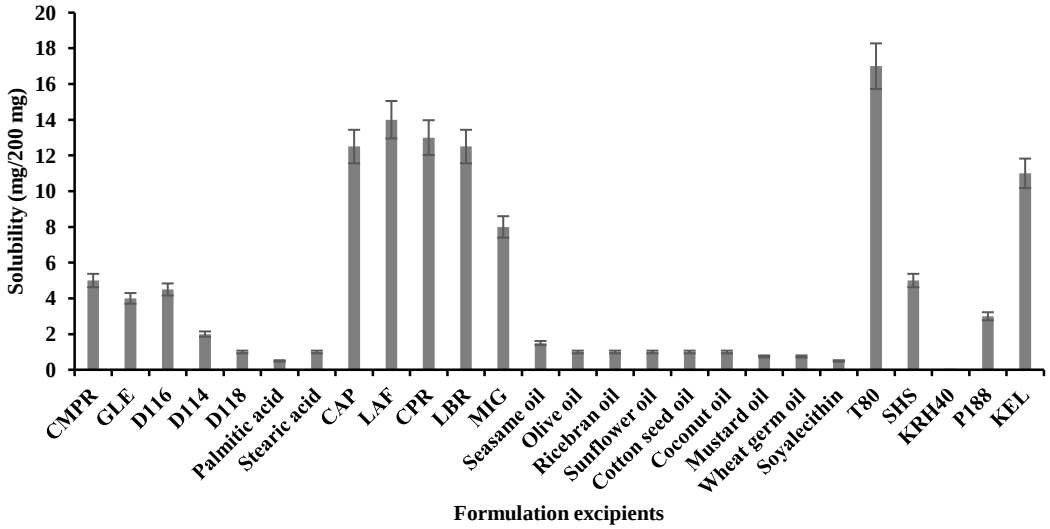

Fig. 2. Solubility of curcumin in formulation excipients

3.1.2 Preliminary screening of formulation and process related parameters

The formulations with GLE and D118 lacked thermodynamic stability (phase separation) and formulations with D114 and D116 showed better particle size but observed drug leakage on storage for 48 h. The CMPR formulation showed higher particle size in comparison with other solid lipids but has a narrow size distribution with a PDI of 0.240. The combination of T80 and SHS gave smaller particle sizes as compared to the individual emulsifiers when used alone. Thermodynamic stability was improved with non-ionic emulsifiers (alone or in combination). To reduce the toxicity of individual emulsifiers due to high concentration, a combination of emulsifiers was used at low concentrations. It was observed that as the emulsifier concentration was increased, the particle size and PDI decreased. The smallest particle size was obtained with 2 %w/v emulsifier concentration, but it was comparable with that obtained with 1.5 %w/v. As a result, 1.5 percent of the emulsifier concentration was chosen. The least particle size and PDI were observed when the curcumin NLCs were subjected to 15 min of sonication. High sonication time may increase the energy of the system, making it unstable. However, there was no significant difference in particle size and PDI obtained from 10 and 15 min of sonication, so 10 min was chosen as the sonication time for the subsequent series of experiments (Table 4).

Table 4. Preliminary screening data for formulation and process related parameters of curcumin loaded NLCs

Variable	SL	LL	Emulsifier	EC	ST	Particle size (nm)	PDI	Thermodynamic stability
SL	CMPR	CAP	T80	1.5	10	348.7 ± 9.4	0.240 ± 0.009	YES
	GLE	CAP	T80	1.5	10	284.4 ± 41.3	0.280 ± 0.088	NO
	D116	CAP	T80	1.5	10	316.6 ± 21.8	0.310 ± 0.074	NO
	D114	CAP	T80	1.5	10	297.7 ±	0.340 ±	NO

						9.8	0.038	
	D118	CAP	T80	1.5	10	272.5 ± 7.6	0.290 ± 0.021	NO
	CMPR	CAP	T80	1.5	10	358.4 ± 11.5	0.350 ± 0.010	YES
Emulsifier	CMPR	CAP	SHS	1.5	10	322.3 ± 11.4	0.310 ± 0.012	YES
	CMPR	CAP	T80+SHS	1.5	10	307.7 ± 10.9	0.280 ± 0.009	YES
	CMPR	CAP	T80+SHS	1.5	5	398.1 ± 6.4	0.470 ± 0.099	NO
ST	CMPR	CAP	T80+SHS	1.5	10	312.4 ± 4.9	0.340 ± 0.008	YES
	CMPR	CAP	T80+SHS	1.5	15	301.9 ± 16.7	0.280 ± 0.021	YES
	CMPR	CAP	T80+SHS	1.0	10	463.9 ± 58.9	0.510 ± 0.120	NO
EC	CMPR	CAP	T80+SHS	1.5	10	313.4 ± 11.6	0.360 ± 0.010	YES
	CMPR	CAP	T80+SHS	2.0	10	287.8 ± 7.9	0.290 ± 0.008	YES

SL-Solid lipid, LL-Liquid lipid, EC-Emulsifier concentration in (%w/v), ST-Sonication time in min, PDI-Polydispersity index.

3.1.3 Optimization (Design of experiment)

The effects of the specified parameters, EC and ST, on particle size and PDI are shown in Table 5.

Table 5. Responses observed in 2^2 factorial design for curcumin loaded NLCs

Runs	Batch Code	Factor 1: EC		Factor 2: ST		Dependent variable/responses	
		Level	mg	Level	min	Response 1 PS (nm)	Response 2 PDI
1	F1	-1	130	-1	7	570.3	0.522
2	F2	-1	130	-1	7	553.8	0.533
3	F3	+1	180	-1	7	491.8	0.423
4	F4	+1	180	-1	7	503.1	0.422
5	F5	-1	130	+1	12	459.8	0.322
6	F6	-1	130	+1	12	450.0	0.326
7	F7	+1	180	+1	12	301.2	0.283
8	F8	+1	180	+1	12	299.4	0.276

3.1.3.1 Response 1: Particle size

The Particle size of the lipid nanoparticle formulations prepared varied from 570 nm to 299 nm. From the data in Table 5, it is clear that particle size depends upon both EC and ST used in preparation and was found to be statistically significant at $p<0.05$. Table 6. indicates the result of ANOVA provided by the software after feeding the response of particle size.

The following parameters were deduced by the software for this response particle size:

- The Model F-value of 427.45 implies the model is significant. There is only a 0.01% chance that a "Model F-Value" this large could occur due to noise.
- Values of "Prob > F" less than 0.0500 indicate model terms are significant. In this case, A, B and AB are significant model terms.
- The "Pred R-Squared" of 0.9876 is in reasonable agreement with the "Adj RSquared" of 0.9946.
- "Adeq Precision" measures the signal to noise ratio. A ratio greater than 4 is desirable. Your ratio of 48.605 indicates an adequate signal. This model can be used to navigate the design space.

The factorial equation for determining particle size: Particle size = 453.93 - 55.05 A - 75.83 B - 22.75 AB

The data clearly indicates that the particle size is strongly dependent on the selected independent variables. The fitted equation relating the response (particle size) to the transformed factor is shown by the above equation.

Polynomial equations can be used to draw conclusions after considering the magnitude of the coefficient and the mathematical sign it carries (i.e., positive or negative). The above equation represents the effects of individual and combined variables on the particle size of curcumin-loaded NLCs. The equation suggests that the factors A, B, and AB have a negative effect on particle size. Negative value coefficients of A, B, and AB indicate that particle size increases with a decrease in the EC and ST. When the coefficient values of two independent key variables (A and B) are compared, the value of the coefficient of the combined variable AB (-22.75) was found to be lower than that of the individual variables A and B. Hence, EC and ST were considered to be major contributing variables for the particle size of curcumin loaded NLCs.

Effect of EC: Variation in the EC has significantly affected the particle size of the formulation ($p<0.05$). The observed particle size decreased significantly with an increase in EC. The possible reason is due to rapid stabilization of nanoparticles at high EC. At lower EC, stabilization of nanoparticles is limited, causing an increase in particle size. Therefore, the increase in the EC decreases the particle size and hence improves stability.

Effect of ST: The ST will influence the particle size of the nanoparticles, as the particle size is inversely proportional to the ST. This is attributed to the ultra-sonication energy provided for the breaking of the emulsion into smaller sizes.

In the present study, when the ST was varied from 7 to 12 min, the particle size decreased irrespective of the EC ($p<0.05$). Thus, the particle size was further decreased by increasing the ST at the optimal EC level.

Contour and 3D response surface plots: The relationship between the dependent and independent variables was further elucidated using the contour and response surface plots. 3D response surface plots give a representation of the variations in each response when the two factors are simultaneously changed from a lower to a higher level. It gives a three dimensional curvature of the change in response at different factor levels. It also gives the variation in design points from the predicted response value. The response surface 3D plot (Fig. 3A) illustrates the finding that as the amount of emulsifier was increased, particle size decreased. The same observations were also indicated by the contour plot (Fig. 4A).

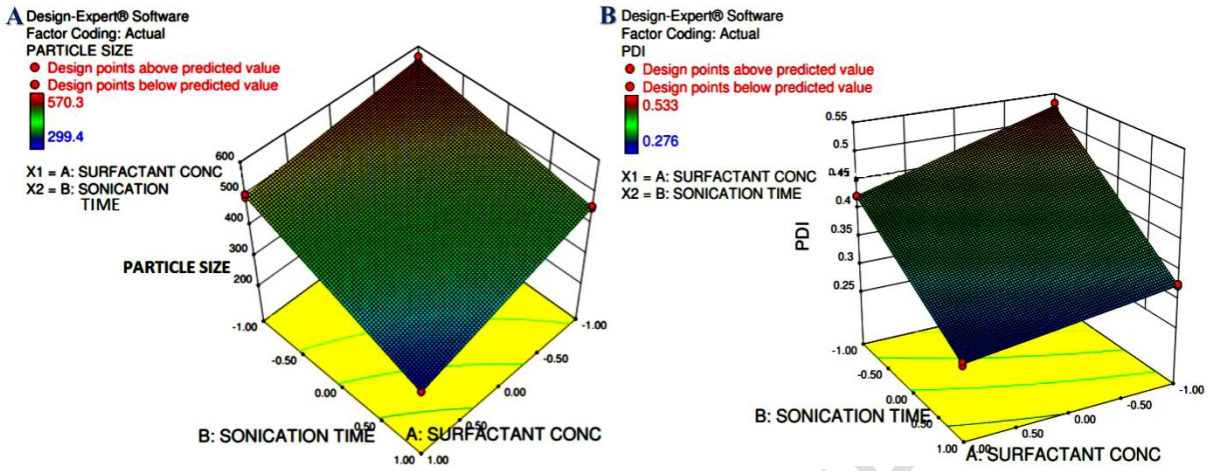

Fig. 3. 3D Surface response plot for (A) particle size, (B) PDI

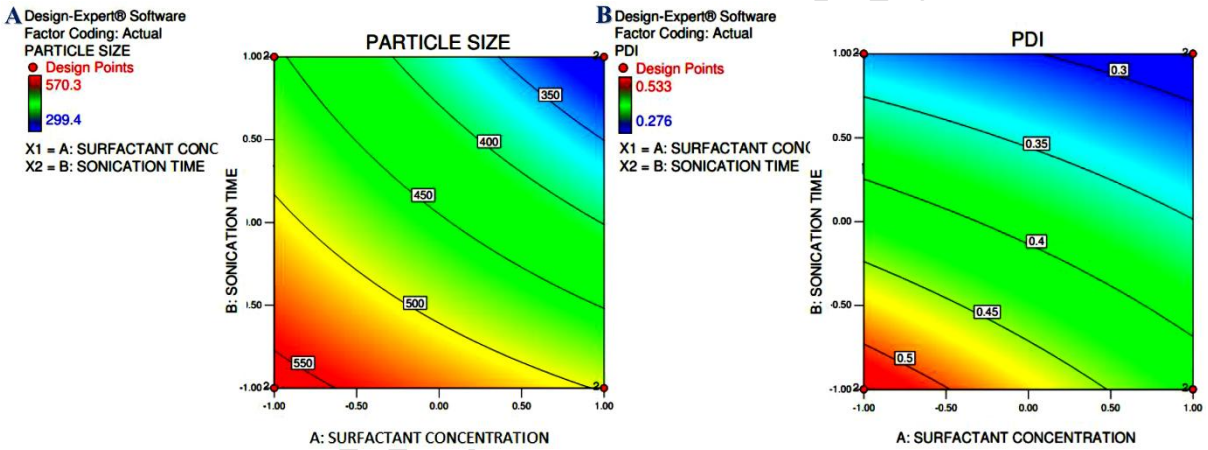

Fig. 4. Contour plot for (A) particle size, (B) PDI

3.1.3.2 Response 2: PDI

The PDI of curcumin loaded NLC formulations varied from 0.53 to 0.27 and was found statistically significant at $p<0.05$. From the data in Table 5, it is clear that PDI depends upon both EC and ST. Table 6. indicates the data provided by the software after feeding in the result of PDI.

The following parameters were deduced by the software for this response PDI:

- The model F-value of 1041.52 implies the model is significant. There is only a 0.01% chance that a "Model F-Value" this large could occur due to noise.
- Values of "Prob > F" less than 0.0500 indicate model terms are significant. In this case, A, B, and AB are significant model terms.
- The "Pred R-Squared" of 0.9949 is in reasonable agreement with the "Adj RSquared" of 0.9978.
- "Adeq Precision" measures the signal to noise ratio. A ratio greater than 4 is desirable. The ratio of 72.542 indicates an adequate signal. This model can be used to navigate the design space.

The factorial equation derived for PDI: PDI = 0.39 - 0.037A - 0.087B + 0.015 AB

The data clearly indicated that the PDI values are strongly dependent on the selected independent variables. The above equation represents the effects of individual and combined variables on the PDI of a curcumin-loaded NLC formulation. The p-value of less than 0.05 indicates that EC and ST have a significant effect on PDI. On increasing the value of ST (B), a decrease in PDI was observed, because coefficients of B bear a negative sign and are close to zero. The equation also suggested that the factor A has a negative effect on PDI. When the coefficient values of two independent key variables (A and B) are compared, the value of the co-efficient of the combined variable AB (0.015) was found to be greater than that of A and B, and hence EC and ST were considered to be a major contributing variable for PDI in NLCs.

Effect of the EC: The EC played an important role in the PDI of NLC formulations. The variation in the EC significantly affected PDI ($p<0.05$). The observed PDI decreased significantly when the concentration of emulsifier increased.

Effect of the ST: The ST played a very important role in PDI in NLC formulation. On increasing ST, i.e., variable B, a simultaneous decrease in PDI was observed, because coefficients of B bear a negative sign.

Contour and 3D response surface plots: The relationship between the dependent and independent variables was further elucidated using contour and 3D response surface plots. The response surface 3D plot (Fig. 3B), shows that as the amount of emulsifier and ST was increased, the PDI of the formulations decreased. The contour plot (Fig. 4B) also shows that the high levels of EC and ST indicate a decrease in PDI.

Table 6. Results of ANOVA for the response particle size and PDI

Source	ANOVA for the response particle Size			ANOVA for the response PDI		
	F Value	p-value Prob> F	Outcome	F Value	p-value Prob> F	Outcome
Model	427.45	<0.0001	Significant	1041.52	<0.0001	Significant
A: EC	417.98	<0.0001		478.08	<0.0001	
B: ST	792.99	<0.0001		2568.18	<0.0001	
AB	71.38	0.0011		78.29	0.0009	

Overlay plot: The Design Expert® software generated an overlay plot (Fig. 5A) to determine ST and EC, so as to have a minimum particle size and PDI. The overlay plot shows multiple outcomes which were closer to the variables of Batch F8 to give the optimum EC and ST. The overlay plot generated the solution at the level of variable A and B as +1, which is a high level, giving a particle size of 300.3 nm and a PDI of 0.280.

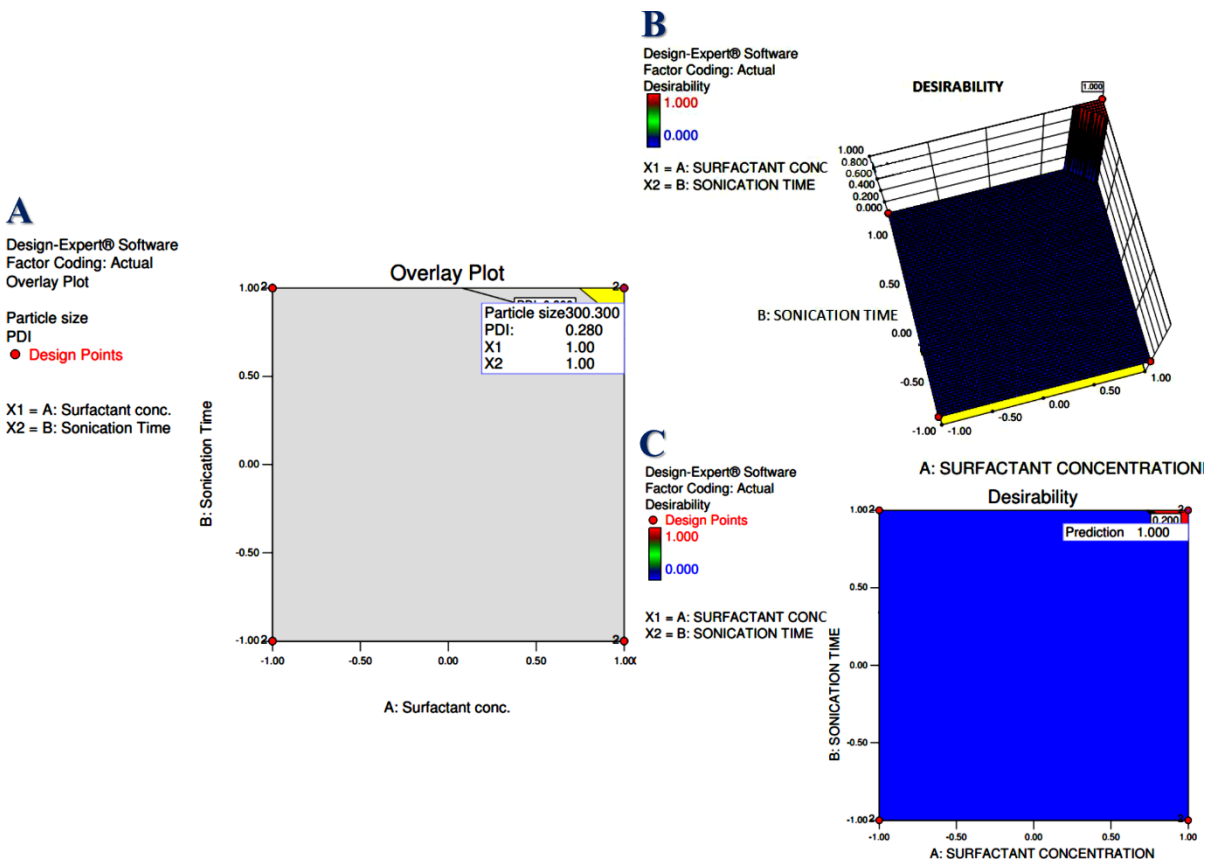

Fig. 5. (A) overlay plot, (B) 3D desirability plot, (C) desirability plot

Optimized batch of NLCs: For the present study, the criteria for the optimum batch were decided as the ones which show minimum particle size and PDI. Based on the response surface model design batches and their response graphs, 30 solutions were suggested by Design-Expert® (Table 7). From desirability plot (Fig. 5B and 5C), it is clear that the desirability value of solution No. 1, i.e., corresponding to batch F8, is closer to unity. Hence, the formulation F8 is considered the optimized formulation.

Table 7. 33 solutions for optimized batch were suggested by Design-Expert®

No.	SC	ST	Particle size (nm)	PDI	Desirability
1	1.00	1.00	300.300	0.279500	1.000
2	0.89	0.89	319.214	0.289868	1.000
3	0.84	0.93	319.234	0.287985	1.000
4	0.92	0.87	319.013	0.290532	1.000
5	0.89	0.95	313.648	0.285431	1.000
6	0.95	0.90	313.706	0.287688	1.000
7	0.98	0.93	308.685	0.284786	1.000
8	0.91	0.94	312.927	0.285858	1.000
9	0.87	0.92	318.550	0.288562	1.000
10	0.94	0.94	311.238	0.285394	1.000
11	0.79	0.99	317.782	0.285146	1.000
12	0.92	0.88	317.886	0.289940	1.000

13	0.87	0.94	316.129	0.286639	1.000
14	1.00	0.98	302.717	0.281124	1.000
15	0.95	0.95	308.861	0.284077	1.000
16	0.90	0.91	317.152	0.288468	1.000
17	0.94	0.96	308.113	0.283313	1.000
18	0.87	0.97	312.950	0.284363	1.000
19	0.98	0.88	313.085	0.288279	1.000
20	0.94	0.91	314.093	0.287664	1.000
21	0.89	0.97	312.007	0.284318	1.000
22	0.93	0.99	306.966	0.281964	1.000
23	0.94	0.95	309.348	0.284151	1.000
24	1.00	0.87	313.347	0.288927	1.000
25	0.91	0.89	318.390	0.289841	1.000
26	0.83	0.96	316.663	0.285899	1.000
27	0.86	0.94	316.833	0.286833	1.000
28	0.90	0.88	319.452	0.290323	1.000
29	0.97	0.90	312.460	0.287511	1.000
30	0.85	0.92	319.601	0.288596	1.000

Composition of optimized batch: With an EC of 180 mg and ST of 12 min, batch Code No. F8 is chosen as the optimized formulation that has the lowest particle size of 300.3 nm, with a PDI of 0.28.

3.1.4 Lyophilization

It was found that all the formulations with cryoprotectants were readily redispersible (Table 8). Dextrose at 7% w/v concentration gave maximum stability of the NLCs after freeze drying, with a minimal increase in particle size. Mannitol at 10% w/v gave a smaller particle size than the other concentration of mannitol used, but the particle size was very large as compared to the initial formulation (Fig. 6). Sucrose gave better results at 10% w/v as compared to lower concentrations.

Fig. 6. (A) curcumin loaded NLCs, (B) lyophilized curcumin loaded NLCs

Table 8. Screening of cryoprotectants for Lyophilization

Cryoprotectants	Concentration (%)	Initial particle size (nm)	Redispersed NLCs		Sf/Si Ratio	Redispersibility grade
			Particle size (nm)	PDI		
Curcumin	--	298.5 ±	1217.8 ± 128.9	0.891 ± 0.110	4.08	C

NLCs		9.3				
	5	(PDI 0.287	489.9 ± 41.8	0.560 ± 0.089	1.64	A
Dextrose	7	± 0.011)	332.8 ± 5.9	0.350 ± 0.007	1.11	A
	10		674.6 ± 55.3	0.490 ± 0.037	2.26	A
	5		647.7 ± 54.7	0.673 ± 0.029	2.17	A
Sucrose	7		589.7 ± 103.1	0.831 ± 0.085	1.98	A
	10		503.7 ± 28.1	0.331 ± 0.021	1.69	A
	5		1056.9 ± 200.1	0.896 ± 0.098	3.54	B
Mannitol	7		749.9 ±128.6	0.884 ± 0.112	2.51	A
	10		708.6 ± 78.9	0.611 ± 0.035	2.38	A

3.2 Characterization and evaluation of lyophilized curcumin loaded NLCs

3.2.1 Redispersibility and drug content

After adding water, the formulation reconstituted quickly and readily. With manual shaking, the formulation was found to be easily redispersible. The drug content in the formulation was found to be 99.12 ± 1.43 %. The chromatogram of the standard curcumin (Fig. 7A) and curcumin in the curcumin loaded NLC formulation (Fig. 7B) was comparable. This shows that the drug does not undergo degradation when formulated in the form of NLCs.

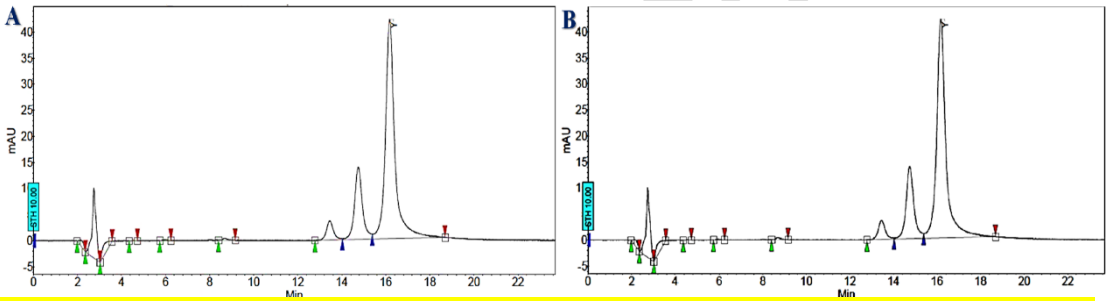

Fig. 7. Chromatogram of (A) standard curcumin, (B) curcumin in curcumin loaded NLCs

3.2.2 Particle size, size distribution and zeta potential

The particle size of the curcumin loaded NLCs dispersion was 298.5 ± 9.3 nm with a polydispersity index of 0.287 ± 0.011, whereas the optimized lyophilized curcumin loaded NLCs were 332.8 ± 5.9 nm with a PDI of 0.350 ± 0.007, respectively. The particle size and PDI of the NLCs tend to increase on lyophilization. The Sf/Si ratio (ratio of nanoparticle size after and before lyophilization) of 1.11 was observed, which can be considered acceptable. Though the PDI of lyophilized products was increased, it was within the acceptable limit. The T80 and SHS stabilized NLC formulations had a zeta potential value of 0.072 ± 0.005 mV. Both the emulsifiers are non- ionic and do not bear any charge. Hence, the particles did not show any surface charge on them. Also, the lyophilized formulation had a zeta potential value of 0.098 ± 0.019 mV, which is not a very significant change. Hence, lyophilization did not affect the zeta potential of the formulation.

3.2.3 Entrapment efficiency and drug loading

The entrapment of curcumin loaded NLCs and redispersed NLCs was found to be 98.42 ± 0.96 % and 97.64 ± 1.59 % respectively, suggesting the maximum amount of drug entrapment in the NLCs. The curcumin-loaded NLCs had a drug loading of 2.50 ± 0.16%.

3.2.4 Surface morphology

SEM studies suggest the irregular shape of the curcumin loaded NLCs with smooth surface morphology (Fig. 8A). The cryoprotectant was also found to be irregular in shape with aggregated masses (Fig. 8B). SEM of lyophilized formulation showed adsorption of irregular particles of NLCs on the surface of cryoprotectant (Fig. 8C). Also, the particle size observed using SEM was found to be in agreement with that obtained from the particle size analyzer. The picture depicts the agglomeration of some individualized particles due to the lipid nature of the carriers and sample preparation prior to SEM analysis.

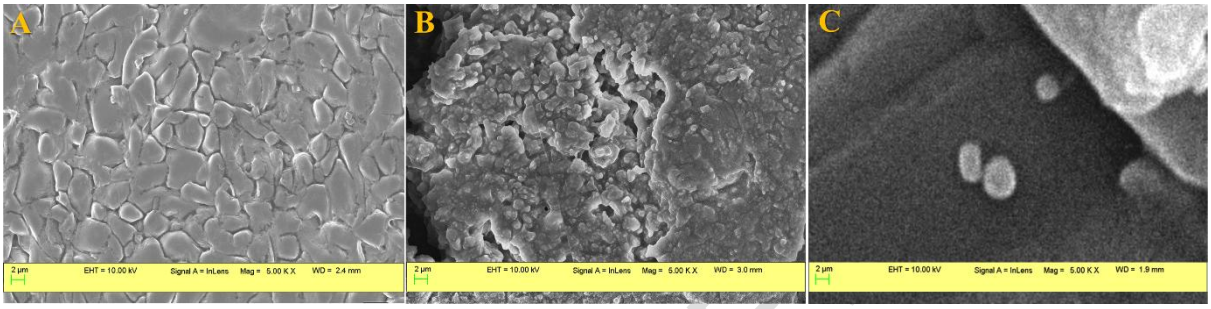

Fig. 8. Surface morphology of (A) curcumin loaded NLCs (formulation), (B) dextrose (Cryoprotectant) and (C) lyophilized curcumin loaded NLCs (formulation)

3.2.5 Crystallinity studies

Curcumin powder was highly crystalline as evident from sharp peaks seen at the 2θ value of 8, 9.7, 16.5, 18.2 and 20.4 along with some other peaks of lower intensity which are decreased in redispersed curcumin loaded NLCs. The solid lipid CMPR showed broad peaks. The crystalline structure of the lipid slightly changed after the formation of nanoparticles. This indicated that encapsulation of curcumin in the lipid matrix of NLCs did not influence lipid matrix structure. XRD of curcumin loaded NLCs confirmed that the individual components have partially lost their crystalline nature when incorporated into NLC (Fig. 9).

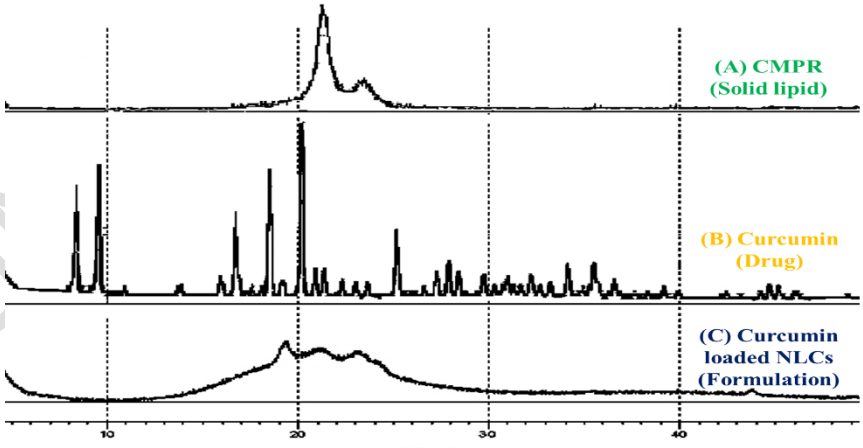

Fig. 9. XRD analysis of (A) CMPR (solid lipid), (B) curcumin (drug), (C) curcumin loaded NLCs (formulation)

3.2.6 Thermal behavior

Melting point of pure CMPR was detected at 77.62 °C. Curcumin showed sharp endotherm with melting point of 176.34 °C. Curcumin, in particular, showed a reduction of the endothermic peak at 161.96 °C and CMPR showed a broad endothermic peak at 89.26 °C. It was found that curcumin loaded NLCs exhibited a reduction of endothermic peak at 73.78 °C, which corresponds to CMPR. The increased melting range for formulation premix compared to solid lipid could be correlated with less ordered crystals or amorphous state. The absence of the curcumin peak indicated that curcumin had been incorporated into the NLC lipid matrix (Fig. 10).

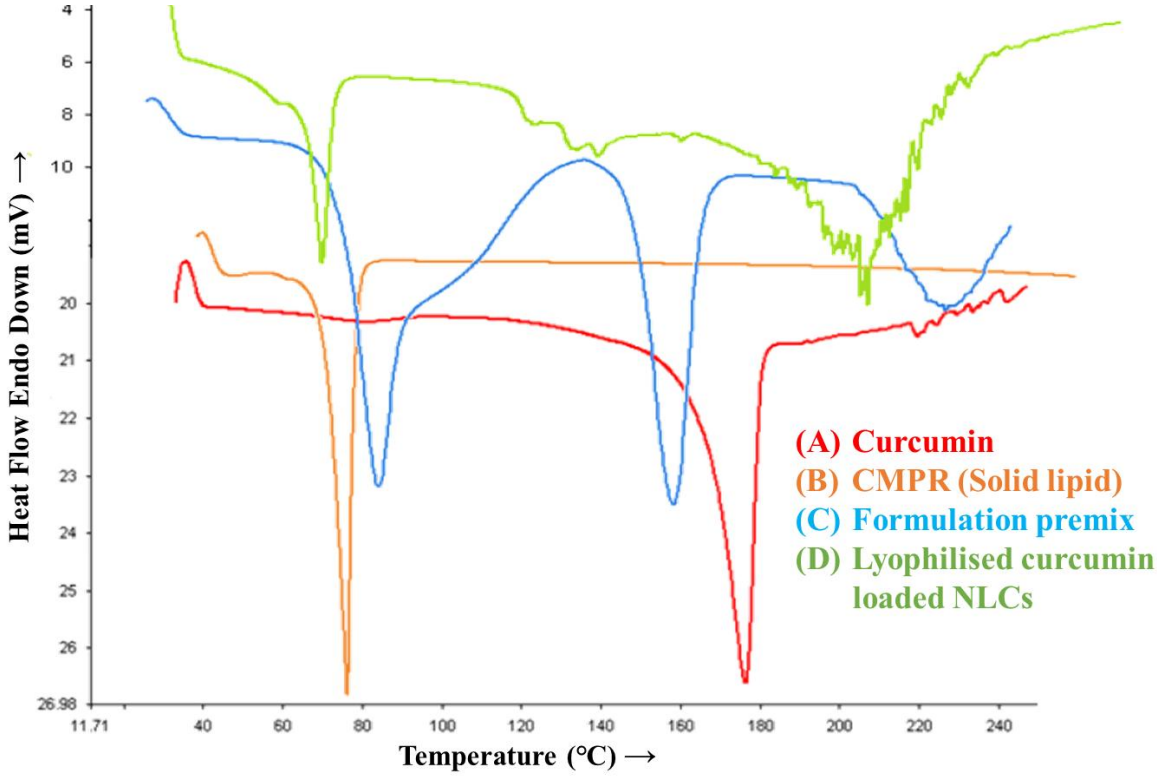

Fig. 10. Endotherm of (A) curcumin (drug), (B) CMPR (solid lipid), (C) formulation premix, (D) lyophilized curcumin loaded NLCs (formulation)

3.2.7 *In-vitro* drug release studies

For *in-vitro* dissolution of a hydrophobic drug, sink conditions were to be maintained to achieve maximum release of the drug. The drug was poorly soluble in phosphate buffer saline; hence, it was required to develop a dissolution medium allowing maximum solubility of the drug. *In-vitro* drug release studies of curcumin loaded NLC formulations were performed to observe the amount of drug released and the pattern of drug release from the nanoparticles. It was observed that 98.30 ± 0.81 % of curcumin from the curcumin suspension was released at the end of 6 h, whereas only 34.49 ± 1.35 % of the curcumin from the formulation was released at the same time. At the end of 24 h, the drug release from the formulation was found to be 51.29 ± 2.11 %. The drug release from curcumin suspension was very fast, whereas the cumulative release rate from the formulation was much slower; an initial burst release was followed by a sustained release. The drug release profile of redispersed NLCs was comparable to that of the curcumin loaded NLC formulation (Fig. 11).

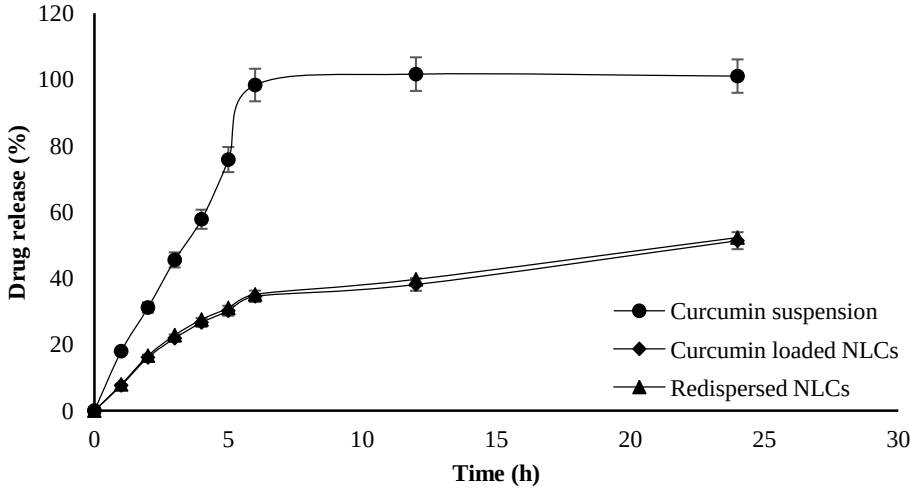

Fig. 11: *In-vitro* drug release profile of curcumin suspension, curcumin loaded NLCs and redispersed curcumin loaded NLCs

The *in-vitro* release profiles of drugs from the formulation could be best expressed by the Higuchi model as the plots showed the highest linearity (R^2=0.8901) than the other plots (Fig. 12). It confers that drugs are released by diffusion. Thus, the formulation complied very well with the assumptions of the Higuchi model that are, (i) the drug concentration in the matrix is initially much higher than the solubility of the drug; (ii) the thickness of the dosage form is much larger than the size of the drug molecules. To determine the mechanism of drug release from the curcumin-loaded NLC formulation, the *in-vitro* drug release data were fitted to Korsmeyer-peppas. The formulation F8 was found to have good linearity (R^2 = 0.9892) and a slope, i.e. the diffusion component (n), of 0.3484, indicating that fickian diffusion was the dominant mechanism of drug release from the formulation.

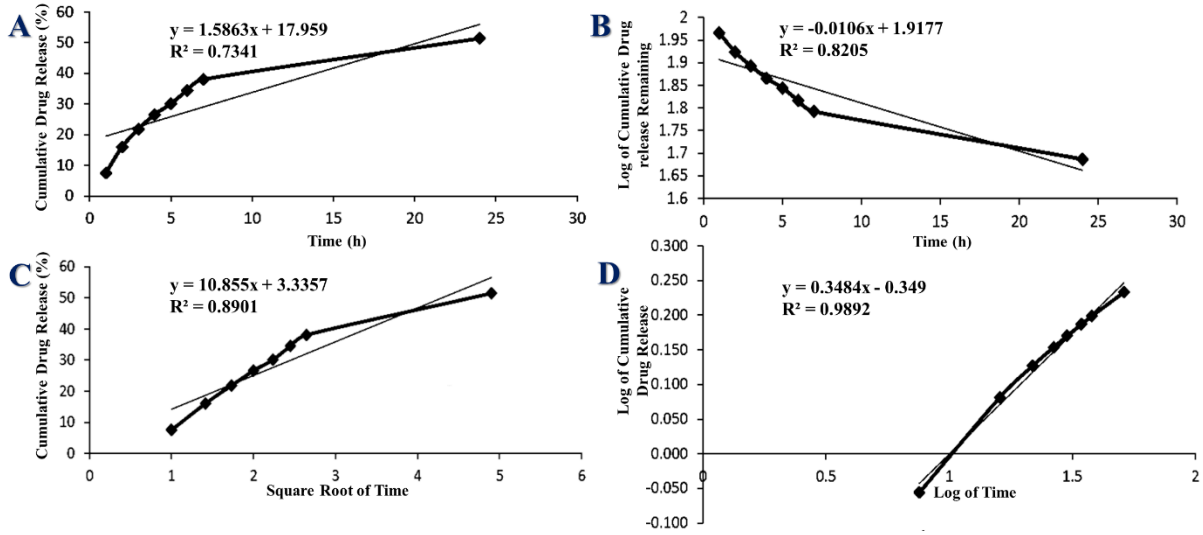

Fig. 12: Release kinetics of curcumin loaded NLCs (A) zero order release, (B) first order release, (C) Higuchi release and (D) Korsmeyer- peppas.

3.3 *In-vitro* cytotoxicity study for curcumin loaded NLCs

Fig. 13. represents the % control growth and the growth curve, and Table 9. enlists the LC_{50}, TGI, and GI_{50} values of the samples calculated from the graph. Fig. 14. illustrates images showing cell cytotoxicity of samples against the A-549 cell line A growth percent of 100 corresponded to growth seen in untreated cells. A growth percent of 0 indicated no net growth over the course of the assay (i.e. equal to the number of cells at time zero). Growth percent of -100 resulted when all the cells were killed. Three endpoints were routinely calculated: 1) GI_{50}, which is the log M concentration yielding a growth percent of 50 (i.e., 50% growth inhibition), 2) TGI, which is the log M concentration yielding a growth percent of 0, or total growth inhibition, and 3) LC_{50}, which is the log M concentration yielding a growth percent of 50, or lethality in 50% of the starting cells. From the graph, it could be observed that the curcumin loaded NLC formulation showed a maximum decrease in the percent growth of the cells. The curcumin in DMSO was almost as efficient as the positive control. Curcumin in water showed no or very little decline in percent cell growth as the drug is very poorly soluble in water and hence might not be available to cause the desired activity. The NLCs formulation and ADR showed TGI, GI_{50} and LC_{50} at concentrations below 10 µg/ml. The curcumin in DMSO showed LC_{50} and TGI at concentrations above 40 µg/ml. The results obtained from curcumin in water were not equivalent, though, as suggested by the studies. This result could be due to less solubility of the compound. A GI_{50} value of ≤ 10^-6 mol (i.e. 1 µmol) or ≤ 10 µg/ml was considered to demonstrate activity in the case of pure compounds. As a result, curcumin loaded NLC formulation, curcumin suspended in water, and curcumin in DMSO all demonstrated activity against the cell lines. Hence, it can be concluded that curcumin loaded NLCs showed improved effectiveness in preventing cell growth as compared to curcumin in water and DMSO.

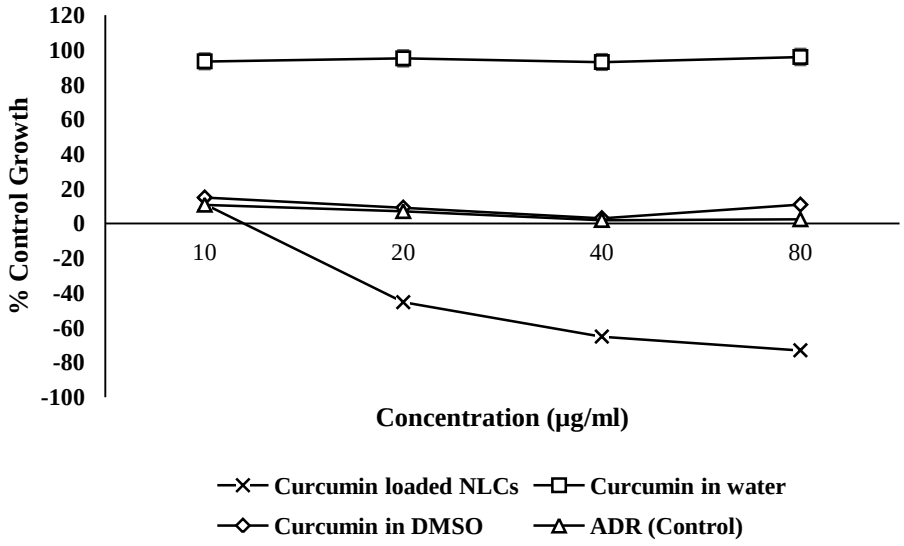

Fig. 13. Growth curve of samples against A-549 curcumin loaded NLCs, curcumin in water, curcumin in DMSO, ADR

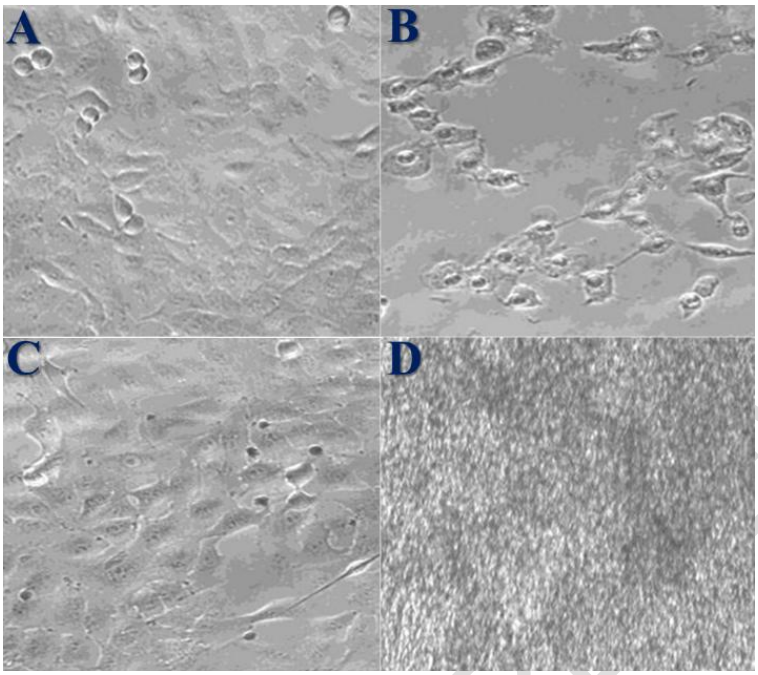

Fig. 14. Cell cytotoxicity of samples against A-549 cell line (A) curcumin loaded NLCs (formulation), (B) curcumin in water, (C) curcumin in DMSO and (D) ADR (A-549 positive control)

Table 9. LC_{50}, TGI and GI_{50} values of the samples

A-549 cell line	LC_{50}	TGI	GI_{50}
Curcumin loaded NLCs	<10	<10	<10
Curcumin in water	Not equivalent	Not equivalent	Not equivalent
Curcumin in DMSO	>40	>40	<10
ADR (Control)	<10	<10	<10

3.4 Real-time stability studies

The stability study results suggested that the formulation was quite stable for the study duration of 90 d. There were no significant changes in the particle size, PDI, and zeta potential. Also, the appearance was similar to that observed on the initial day. The formulation was easily redispersible throughout the batches. There was no change in EE and drug content. The *in-vitro* release profile of the formulation suggested a constant release pattern of the drug by indicating the stability of the NLC formulation (Fig. 15). It was observed that the formulation was stable when kept in refrigerated conditions as well as to room temperature (Table 10). All the parameters were within acceptable limits, which showed that the formulations were stable over a period of 90 d. The results of stability studies indicated that the formulation had reasonable stability and would be acceptable for regulatory submissions where stability is paramount for any formulation.

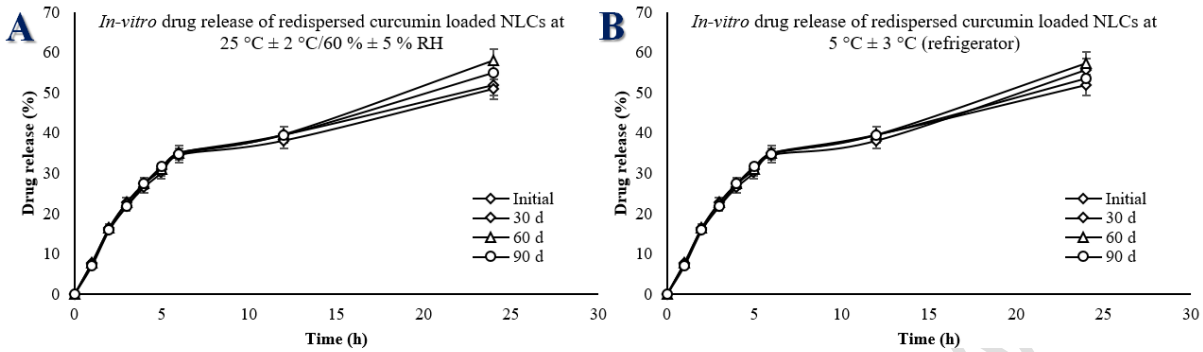

Fig.15. *In-vitro* drug release profile of curcumin loaded NLCs stability at 25 °C ± 2 °C/60 % ± 5 % RH and 5 °C ± 3 °C (refrigerator)

Table 10. Stability data of curcumin loaded NLCs subjected to 25 °C ± 2 °C/60 % ± 5 % RH and 5 °C ± 3 °C (refrigerator)

Parameter	Initial	25 °C ± 2 °C/60 % ± 5 % RH			5 °C ± 3 °C (refrigerator)		
		30 d	60 d	90 d	30 d	60 d	90 d
Redispersibility (Grade)	A	A	A	A	A	A	A
Particle size (nm)	332.8 ± 5.9	340.1 ± 11.9	349.2 ± 12.7	348.2 ± 8.4	336.2 ± 4.9	340.6 ± 12.1	342.8 ± 6.5
PDI	0.350 ± 0.007	0.353 ± 0.012	0.368 ± 0.009	0.377 ± 0.019	0.359 ± 0.011	0.365 ± 0.009	0.369 ± 0.018
Zeta potential (Mv)	0.098 ± 0.019	0.088 ± 0.020	0.106 ± 0.014	0.095 ± 0.038	0.094 ± 0.034	0.092 ± 0.027	0.102 ± 0.039
In-vitro drug release (%)	52.01 ± 4.11	50.89 ± 6.79	57.95 ± 7.54	54.88 ± 4.78	55.63 ± 5.68	57.41 ± 3.97	53.47 ± 6.78
EE (%)	97.64 ± 1.59	98.65 ± 1.11	98.69 ± 1.48	98.75 ± 0.87	98.73 ± 0.69	98.64 ± 0.37	98.69 ± 0.98
Drug content (%)	99.12 ± 1.43	99.63 ± 0.45	99.64 ± 0.36	99.54 ± 0.78	99.69 ± 1.87	99.66 ± 0.34	99.61 ± 0.88

4. DISCUSSION

The curcumin showed maximum solubility in CMPR. Chemically CMPR is a mono-, di-, and triesters of behenic acid and GLE is composed of monoglycerides. This decreases the chances of crystallization of lipids into various polymeric forms and thus can encapsulate the maximum amount of curcumin. Further, dynasans (114, 116, and 118) are highly crystalline in nature, which shows minimum solubility for curcumin and limits their encapsulation efficiency [23,24]. The stability of lipid nanoparticles can be improved by incorporating liquid lipid (oil component) as it can control crystal structure. The LAF showed the maximum solubility for curcumin. The encapsulation efficiency can be easily improved by liquid lipids due to the higher solubility of curcumin in liquid lipids. Further, stability of the system can be improved as the surface tension of oil droplets can be controlled better with emulsifiers, which helps to maintain a smaller particle size in the system [25]. The incorporation of emulsifiers helps to reduce particle aggregation, which improves the stability of the system. The combination of non-ionic emulsifiers T80 and SHS were used in curcumin loaded NLCs, which maintains the balance of crystallization by repelling forces. This helps to maintain the

stability of the lipid nanoparticles during the shelf life [26]. The higher emulsifier concentrations provide enough emulsifiers to cover the tiny lipid particles which stabilize and prevent the coalescence of nanoparticles. Lipid systems with low emulsifier concentration lead to aggregation of lipid particles due to hydrophobic attraction between insufficiently covered lipid crystal surfaces [27,28,29]. The results show that the higher emulsifier concentration of 2 % produced NLCs between 300-400 nm with a size distribution of (0.200-0.350). In order to avoid the toxicity of individual emulsifiers at high concentrations, a combination of emulsifiers at low concentrations was used. The individual emulsifier concentration was limited to 0.9 % to avoid toxicity. The particle size and its size distribution can be decreased by increasing the sonication time. The ultra sonication helps to breakdown the coarser lipid particles to the nanoscale. Thus, increased sonication time provides more energy which provides shear stresses and breaks down the particle size. Further, increased sonication time also provides the production of nanoparticles with a very narrow size distribution [30]. The results obtained were in accordance with the published literature. The sonication time of more than 10 min resulted in a particle size around 300 nm with a size distribution less than 0.350. The lyophilized curcumin loaded NLCs showed a slight increase in particle size after Redispersion may be due to the agglomeration of nanoparticles. This could be attributed to the stresses associated with freezing, resulting in a measurable increase in particle size [29, 31]. However, the redispersed curcumin loaded NLCs resulted in a particle size of 332.8 ± 5.9 nm with a size distribution of 0.350 ± 0.007, which is considered not a significant difference from standard curcumin loaded NLCs. Further, it was reported that nanoparticles reach the target site by capillary distribution. These particles can easily cross vascular endothelia and accumulate at the target tumor site by enhanced permeation and retention effects [32]. The hydrophilic polyethylene oxide chains in the T80 provide the stabilizing effect through stearic repulsion. These chains are presumed to form a shell around the nanoparticles that sterically prevents the nanoparticles from aggregation [33]. The release of curcumin from NLCs dispersion was only 34.49 ± 1.35 % in comparison with standard curcumin suspension of 98.30 ± 0.81 % at 6 h. The initial rapid release may be due to the release of curcumin from liquid lipids and from NLCs' surface, whereas the sustained release characteristics suggest the diffusion of drugs from the core of the lipid matrix. Sustained release from NLCs may result in prolonged exposure of tumor cells to this drug, increasing clinical efficacy. The initial rapid release of drug from the nanoparticles is attributed to the drug-enriched oil droplets located on the outer surface of the nanoparticles. The higher melting point of the solid lipid core provides a sustained release matrix for drugs [11]. The curcumin loaded NLCs in the present study showed significant cytotoxicity in comparison with the positive control ADR. The cytotoxic effect of curcumin loaded NLCs is exhibited by a pro-apoptotic effect [10]. The half-maximal inhibitory concentration (IC50) values in the present study showed less than 10 µg/ml for curcumin loaded NLC and ADR (control). The higher IC50 value for curcumin in water may be attributed to the insoluble nature of curcumin in the desired medium. The obtained results were supported by various previously published articles. Madane and Mahajan *et al.* reported that the increased cytotoxic effect of curcumin loaded NLCs against the glioblastoma cell line. The IC50 values were reported to be 9.8 ng/ml for curcumin loaded NLCs and 13.6 ng/ml for ADR (control) [11]. The study of cellular uptake and anticancer efficiency against brain cancer for curcumin NLCs showed an IC50 of 20 mg/ml, which is four times less than standard curcumin. Furthermore, when administered in the NLC system, plasmid concentration showed a 6.4-fold increase in curcumin concentrations, and inhibitory efficiency increased from 19.5% to 82.3% over plan curcumin than in curcumin loaded NLCs [13]. Another study reported that the cytotoxic effect of curcumin loaded NLCs on Hela cells was due to the ability of NLCs to attach and pass through the cell membranes, inducing apoptosis, inhibiting cell proliferation and also inhibiting telomerase activity [15]. The cytotoxicity against human lung adenocarcinoma A549 cells showed a higher apoptosis rate for curcumin loaded NLCs than

standard curcumin. The reported IC 50 value for curcumin loaded NLCs was 5.66 mg/l and 9.81 mg/l for standard curcumin [16].

5. CONCLUSION

The lyophilization of curcumin-loaded NLCs was performed for improved oral administration. In this study, the optimized curcumin-loaded NLCs were developed by a modified hot melt emulsification and characterized as oral formulations. The optimized curcumin-loaded NLCs consist of CMPR as a solid lipid, CAP as a liquid lipid, and a combination of T80 and SHS as emulsifiers. The impact of formulation and process parameters was investigated by a systematic approach in terms of thermodynamic stability, particle size, size distribution, and entrapment efficiency. Further, the thermodynamic stability of the NLC dispersion was improved by lyophilization using 5% mannitol as a cryoprotectant. The results showed that there was no significant difference between the curcumin loaded NLC dispersion and the lyophilized product in particle size, zeta potential, entrapment efficiency, drug loading, and surface morphology. That meant the addition of mannitol in the formulation did not affect the curcumin-loaded NLC dispersion. The optimized NLC formulation has a sustained release profile for curcumin. The curcumin-loaded NLCs had significant cytotoxic activity against the human lung cancer line A-549, with Adriamycin as a positive control. The developed and optimized lyophilized formulation can be further filled into sachets and capsules for oral administration. In conclusion, the above studies provided evidence that NLCs as lipid-based systems were valuable as oral delivery formulations for improved cytotoxic activity of curcumin.

CONSENT (WHERE EVER APPLICABLE)

Not applicable

ETHICAL APPROVAL (WHERE EVER APPLICABLE)

Not applicable

DISCLAIMER:

AUTHORS HAVE DECLARED THAT NO COMPETING INTERESTS EXIST. THE PRODUCTS USED FOR THIS RESEARCH ARE COMMONLY AND PREDOMINANTLY USE PRODUCTS IN OUR AREA OF RESEARCH AND COUNTRY. THERE IS ABSOLUTELY NO CONFLICT OF INTEREST BETWEEN THE AUTHORS AND PRODUCERS OF THE PRODUCTS BECAUSE WE DO NOT INTEND TO USE THESE PRODUCTS AS AN AVENUE FOR ANY LITIGATION BUT FOR THE ADVANCEMENT OF KNOWLEDGE. ALSO, THE RESEARCH WAS NOT FUNDED BY THE PRODUCING COMPANY RATHER IT WAS FUNDED BY PERSONAL EFFORTS OF THE AUTHORS.

REFERENCES

1. Gupta SC, Patchva S, Aggarwal BB. Therapeutic roles of curcumin: lessons learned from clinical trials. AAPS J 2013;15(1):195-218. doi: 10.1208/s12248-012-9432-8.
2. Allegra A, Innao V, Russo S, Gerace D, Alonci A, Musolino C. Anticancer Activity of Curcumin and Its Analogues: Preclinical and Clinical Studies. Cancer Invest 2017;35(1):1-22. doi: 10.1080/07357907.2016.1247166.

3. Shanmugam MK, Rane G, Kanchi MM, Arfuso F, Chinnathambi A, Zayed ME, et al. The multifaceted role of curcumin in cancer prevention and treatment. Molecules 2015;20(2):2728-69. doi: 10.3390/molecules20022728.
4. Kunwar A, Barik A, Mishra B, Rathinasamy K, Pandey R, Priyadarsini KI. Quantitative cellular uptake, localization and cytotoxicity of curcumin in normal and tumor cells. Biochim Biophys Acta 2008;1780(4):673-9. doi: 10.1016/j.bbagen.2007.11.016.
5. Syng-Ai C, Kumari AL, Khar A. Effect of curcumin on normal and tumor cells: role of glutathione and bcl-2. Mol Cancer Ther 2004;3(9):1101-8. PMID: 15367704.
6. Ravindran J, Prasad S, Aggarwal BB. Curcumin and cancer cells: how many ways can curry kill tumor cells selectively? AAPS J 2009;11(3):495-510. doi: 10.1208/s12248-009-9128-x.
7. Shoba G, Joy D, Joseph T, Majeed M, Rajendran R, Srinivas PS. Influence of piperine on the pharmacokinetics of curcumin in animals and human volunteers. Planta Med 1998;64(4):353-6. doi: 10.1055/s-2006-957450.
8. Sharma RA, Steward WP, Gescher AJ. Pharmacokinetics and pharmacodynamics of curcumin. Adv Exp Med Biol 2007;595:453-70. doi: 10.1002/bdd.2136.
9. Liang S, Ji HF. The pharmacology of curcumin: is it the degradation products?. Trends Mol Med 2012;18(3):138-43. doi: 10.1016/j.molmed.2012.01.004.
10. Wang F, Ye X, Zhai D, Dai W, Wu Y, Chen J, et al. Curcumin-loaded nanostructured lipid carrier induced apoptosis in human HepG2 cells through activation of the DR5/caspase-mediated extrinsic apoptosis pathway. Acta Pharm 2020;70(2):227-37. doi: 10.2478/acph-2020-0003.
11. Madane RG, Mahajan HS. Curcumin-loaded nanostructured lipid carriers (NLCs) for nasal administration: design, characterization, and in vivo study. Drug Deliv 2016;23(4):1326-34. doi: 10.3109/10717544.2014.975382.
12. Chanburee S, Tiyaboonchai W. Enhanced intestinal absorption of curcumin in Caco-2 cell monolayer using mucoadhesive nanostructured lipid carriers. J Biomed Mater Res B Appl Biomater 2018:106(2):734-41. doi: 10.1002/jbm.b.33884.
13. Chen Y, Pan L, Jiang M, Li D, Jin L. Nanostructured lipid carriers enhance the bioavailability and brain cancer inhibitory efficacy of curcumin both in vitro and in vivo. Drug Deliv 2016;23(4):1383-92. doi: 10.3109/10717544.2015.1049719.
14. Kamel AE, Fadel M, Louis D. Curcumin-loaded nanostructured lipid carriers prepared using Peceol™ and olive oil in photodynamic therapy: development and application in breast cancer cell line. Int J Nanomedicine 2019;14:5073-85. doi: 10.2147/IJN.S210484.
15. Rabima, Oktamauri A. Characterisation and cytotoxicity assay of curcumin nanostructured lipid carrier on HeLa cells. Earth Environ Sci 2021;667:1-8. doi: 10.1088/1755-1315/667/1/012055
16. Wang F, Chen J, Dai W, He Z, Zhai D, Chen W. Pharmacokinetic studies and anticancer activity of curcumin-loaded nanostructured lipid carriers. Acta Pharm 2017;67(3):357-71. doi: 10.1515/acph-2017-0021.
17. Rapalli VK, Kaul V, Waghule T, Gorantla S, Sharma S, Roy A, et al. Curcumin loaded nanostructured lipid carriers for enhanced skin retained topical delivery: optimization, scale-up, in-vitro characterization and assessment of ex-vivo skin deposition. Eur J Pharm Sci 2020;152:1-56. doi: 10.1016/j.ejps.2020.105438.
18. Arora R, Katiyar SS, Kushwah V, Jain S. Solid lipid nanoparticles and nanostructured lipid carrier-based nanotherapeutics in treatment of psoriasis: a comparative study. Expert Opin. Drug Deliv 2017;14(2):165-77. doi: 10.1080/17425247.2017.1264386.
19. Jain S, Cherukupalli SK, Mahmood A, Gotantla S, Rapalli VK, Dubey SK, et al. Emerging nanoparticulate systems: Preparation techniques and stimuli responsive

release characteristics. J Appl Pharm Sci 2019;9(08):130-43. doi: 10.7324/JAPS.2019.90817.
20. Sonawane R, Harde H, Katariya M, Agrawal S, Jain S. Solid lipid nanoparticles-loaded topical gel containing combination drugs: an approach to offset psoriasis. Expert Opin Drug Deliv 2014;11(12):1833-47. doi: 10.1517/17425247.2014.938634.
21. Panigrahi S, Hirlekar R. A new stability-indicating RP-HPLC method for determination of curcumin: an application to nanoparticulate formulation. Int J Pharm Pharma Sci 2016;8(12):149-55. doi: 10.22159/ijpps.2016v8i12.14473.
22. Behbahani ES, Ghaedi M, Abbaspour M, Rostamizadeh K, Dashtian K. Curcumin loaded nanostructured lipid carriers: In vitro digestion and release studies. Polyhedron 2019;164:113-22. doi: 10.1016/j.poly.2019.02.002.
23. Padhye SG, Nagarsenker MS. Simvastatin Solid Lipid Nanoparticles for Oral Delivery: Formulation Development and in vivo Evaluation. Indian J Pharm Sci 2013:75(5):591-8. doi: 10.4103/0250-474X.122883.
24. Westesen K, Bunjes H, Koch MHJ. Physicochemical characterization of lipid nanoparticles and evaluation of their drug loading capacity and sustained release potential. J Control Release 1997;48(2):223-36. doi: 10.1016/S0168-3659(97)00046-1.
25. Aihua S, Xiaoshu Z, Yanting L, Xinjuan M, Fei H. Novel formulation strategies for improving oral bioavailability of drugs with poor membrane permeation or presystemic metabolism. J Pharm Sci 1993;82(10):979-87. doi: 10.1002/jps.2600821008.
26. Maryam BZ, Akram P. Effect of surfactant concentration on the particle size, stability and potential zeta of beta carotene nano lipid carrier. Int J Curr Microbiol App Sci 2015;4(9):924-32.
27. Helgason T, Awad TS, Kristbergsson K, McClements DJ, Weiss J. Effect of surfactant surface coverage on formation of solid lipid nanoparticles (SLN). J Colloid Interface Sci 2009;334(1):75–81. doi: 10.1016/j.jcis.2009.03.012.
28. Kovacevic A, Savic S, Vuletaa G, Müller RH, Keck CM. Polyhydroxy surfactants for the formulation of lipid nanoparticles (SLN and NLC): effects on size, physical stability and particle matrix structure. Int J Pharm 2011;406(1):163-72. doi: 10.1016/j.ijpharm.2010.12.036.
29. Wolfgang M, Karsten M. Solid lipid nanoparticles Production, characterization and applications. Adv Drug Deliv Rev 2001;47(2):165-96. doi: 10.1016/S0169-409X(01)00105-3.
30. Silva AC, González-Mira E, García ML, Egea MA, Fonseca J, Silva R, et al. Preparation, characterization and biocompatibility studies on risperidone-loaded solid lipid nanoparticles (SLN): high pressure homogenization versus ultrasound. Colloids Surf B Biointerfaces 2011;86(1):158-65. doi: 10.1016/j.colsurfb.2011.03.035.
31. Amis TM, Renukuntla J, Bolla PK, Clark BA. Selection of cryoprotectant in lyophilization of progesterone-loaded stearic acid solid lipid nanoparticles. Pharmaceutics 2020;12(9):1-15. doi: 10.3390/pharmaceutics12090892.
32. Hu FX, Neoh KG, Kang ET. Synthesis and in vitro anti-cancer evaluation of tamoxifen-loaded magnetite/PLLA composite nanoparticles. Biomaterials 2006;27(33):5725-33. doi: 10.1016/j.biomaterials.2006.07.014.
33. Ghorpade K, Shinde S. Design and development of curcumin loaded nanostructured lipid carriers for solubility enhancement. Int J Curr Res 2019;11(01):20-6. doi: 10.24941/ijcr.33214.01.2019.